A rockfall simulation scheme which preserves the stability properties of rotating rocks

Remco Leine*, Giuseppe Capobianco*, Perry Bartelt†, Guang Lu†
*Institute for Nonlinear Mechanics, University of Stuttgart, Germany
†WSL Institute for Snow and Avalanche Research SLF, Davos Dorf, Switzerland

Summary. The stability properties of a freely rotating rigid body are governed by the intermediate axis theorem, i.e. rotation around the major and minor principal axes is stable whereas and rotation around the intermediate axis is unstable. The stability of the principal axes is of importance for the prediction of rockfall. Current numerical schemes for 3D rockfall simulation, however, are not able to correctly represent these stability properties. In this paper we give a proof using Lyapunov functions of an extended intermediate axis theorem, which not only involves the angular momentum equations but also the orientation of the body. Inspired by the stability proof, we present an novel scheme which respects the stability properties of a freely rotating body and which can be incorporated in numerical schemes for the simulation of rigid bodies with frictional unilateral constraints.

Introduction

A full 3D simulation technique for rockfall dynamics, taking rock shape into account and using the state-of-the-art methods of multibody dynamics and nonsmooth contact dynamics, has been developed in [3]. The rockfall simulation technique is based on the nonsmooth contact dynamics method with hard contact laws. The rock is modeled as an arbitrary convex polyhedron and the terrain model is based on a high resolution digital elevation model. The developed numerical methods have been implemented in the code RAMMS::ROCKFALL, which is being actively used in the natural hazards research community, and is to date the only 3D code which takes rockshape into account [2].
Field observations of natural rockfall events as well as high precision measurements with instrumented experimental rocks [1] have shown that platy disk-shaped rocks have the tendency to roll and bump down the slope around their major principal axis[1]. Simulations with the present implementation of RAMMS::ROCKFALL, however, fail to represent the observed rolling phenomenon.
The intermediate axis theorem is a result of the Euler equations describing the movement of a rigid body with three distinct principal moments of inertia. The theorem describes the following effect: rotation of a rigid body around its minor and major principal axes is stable, while rotation around its intermediate principal axis is unstable. The classical intermediate axis theorem, however, only involves the Euler equations for the three components of the angular velocity. In this paper, we describe the dynamics of a freely rotating body in state-space form using as states the three angular velocity components and an arbitrary parametrization of the orientation of the body with respect to the inertial frame. Using the method of Lyapunov functions we rigorously prove an extended version of the intermediate axis theorem in the full state-space.
In this paper we will show that the present scheme, which is fully explicit during flight phases of the rock, does not respect the intermediate axis theorem. Furthermore, we will present an alternative implicit scheme which correctly describes the stability properties of a freely rotating body.

Equations of motion of a free spinning body

Let $\mathcal{V}$ be the Euclidean vector space. To describe the orientation of the rock, we will use a body-fixed frame $K = (\vec{e}_x^K, \vec{e}_y^K, \vec{e}_z^K)$ as well as an inertial frame $I = (\vec{e}_x^I, \vec{e}_y^I, \vec{e}_z^I)$. An arbitrary vector $\vec{a} \in \mathcal{V}$ can be expressed in the K-frame through the tuple ${}_K\vec{a} \in \mathbb{R}^3$, which is related to its representation ${}_I\vec{a}$ in the inertial frame through

$$\vec{a} = \boldsymbol{A}_{IK}\, {}_K\vec{a}, \tag{1}$$

where $\boldsymbol{A}_{IK} = \begin{pmatrix} {}_I\vec{e}_x^K & {}_I\vec{e}_y^K & {}_I\vec{e}_z^K \end{pmatrix} \in \mathrm{SO}(3)$ is the transformation matrix describing the orientation of the rock. Let ${}_K\vec{\boldsymbol{\Omega}}$ denote the angular velocity of the body expressed in the body-fixed frame K. The spin of the body is defined by

$$\vec{\boldsymbol{N}}_S = \boldsymbol{\Theta}_S\, \vec{\boldsymbol{\Omega}} \tag{2}$$

where $\boldsymbol{\Theta}_S$ is the inertia tensor. The inertia tensor takes a constant form in the body-fixed frame, which we choose to be aligned along the principal axes of inertia, such that

$$\boldsymbol{\Theta} := {}_K\boldsymbol{\Theta}_S = \begin{pmatrix} A & 0 & 0 \\ 0 & B & 0 \\ 0 & 0 & C \end{pmatrix} \tag{3}$$

where $A, B, C > 0$ are the principal moments of inertia around the minor, intermediate and major axis respectively. We will denote $\boldsymbol{\Theta} := {}_K\boldsymbol{\Theta}_S$ as inertia matrix to have a short-hand notation. During flight, the rotational motion of the rock is decoupled from the translational motion and fully described by the spin invariance $\dot{\vec{\boldsymbol{N}}}_S = \vec{\boldsymbol{0}}$, yielding

$${}_K\dot{\vec{\boldsymbol{N}}}_S + {}_K\vec{\boldsymbol{\Omega}} \times {}_K\vec{\boldsymbol{N}}_S = \vec{\boldsymbol{0}} \tag{4}$$

[1] https://youtu.be/oWkTfTGeAEo

in the body-fixed frame, which lead to the Euler equations for a freely rotating rigid body

$$\boldsymbol{\Theta}\dot{\boldsymbol{\omega}} + \boldsymbol{\omega} \times (\boldsymbol{\Theta}\boldsymbol{\omega}) = \mathbf{0}. \tag{5}$$

Herein, we used the short-hand notation $\boldsymbol{\omega} = {}_K\vec{\boldsymbol{\Omega}}$. The evolution of the orientation of the body is described by

$$\dot{\boldsymbol{A}}_{IK} = \boldsymbol{A}_{IK}\tilde{\boldsymbol{\omega}}, \tag{6}$$

where $\tilde{\boldsymbol{\omega}}$ is the skew-symmetric matrix such that $\tilde{\boldsymbol{\omega}}\boldsymbol{c} = \boldsymbol{\omega} \times \boldsymbol{c}$ for all $\boldsymbol{c} \in \mathbb{R}^3$. The orientation of the body may be freely parameterized using for instance unit-quaternions $\boldsymbol{q} \in \mathbb{R}^4$ or axis-angle notation ($\boldsymbol{n}$,χ). The matrix differential equation (6) results in a set of ordinary differential equations for the chosen parametrization. If a quaternion $\boldsymbol{q} = (p_0, \boldsymbol{p}^{\mathrm{T}})^{\mathrm{T}}$ representation is used then the rotation matrix is parametrized as

$$\boldsymbol{A}_{IK} = \boldsymbol{I} + \frac{2}{p_0^2 + \boldsymbol{p}^{\mathrm{T}}\boldsymbol{p}}(\tilde{\boldsymbol{p}}\tilde{\boldsymbol{p}} + p_0\tilde{\boldsymbol{p}}) \tag{7}$$

resulting in

$$\dot{\boldsymbol{q}} = \boldsymbol{F}(\boldsymbol{q})\boldsymbol{\omega} \tag{8}$$

with

$$\boldsymbol{F}(\boldsymbol{q}) = \frac{1}{2\|\boldsymbol{q}\|}\begin{pmatrix}\boldsymbol{p}^{\mathrm{T}} \\ \tilde{\boldsymbol{p}} + p_0\boldsymbol{I}\end{pmatrix}. \tag{9}$$

Invariants of motion of the Euler equations

The body has the rotational kinetic energy

$$T = \frac{1}{2}\boldsymbol{\omega}^{\mathrm{T}}\boldsymbol{\Theta}\boldsymbol{\omega} \tag{10}$$

being a constant of motion as, using (5),

$$\frac{\mathrm{d}}{\mathrm{d}t}T = \boldsymbol{\omega}^{\mathrm{T}}\boldsymbol{\Theta}\dot{\boldsymbol{\omega}} = -\boldsymbol{\omega}^{\mathrm{T}}\big(\boldsymbol{\omega} \times (\boldsymbol{\Theta}\boldsymbol{\omega})\big) = 0\,. \tag{11}$$

A second invariant follows from the spin

$${}_I\vec{\boldsymbol{N}}_S = \boldsymbol{A}_{IK}\boldsymbol{\Theta}\boldsymbol{\omega}, \tag{12}$$

which is constant in the inertial frame, i.e.

$$\frac{\mathrm{d}}{\mathrm{d}t}\left({}_I\vec{\boldsymbol{N}}_S\right) = \dot{\boldsymbol{A}}_{IK}\boldsymbol{\Theta}\boldsymbol{\omega} + \boldsymbol{A}_{IK}\boldsymbol{\Theta}\dot{\boldsymbol{\omega}} = \boldsymbol{A}_{IK}\left(\boldsymbol{\omega} \times (\boldsymbol{\Theta}\boldsymbol{\omega})\right) - \boldsymbol{A}_{IK}\left(\boldsymbol{\omega} \times (\boldsymbol{\Theta}\boldsymbol{\omega})\right) = \mathbf{0}. \tag{13}$$

When expressed in the body fixed frame, the spin ${}_K\vec{\boldsymbol{N}}_S$ is not constant but keeps a constant magnitude

$$\frac{\mathrm{d}}{\mathrm{d}t}||{}_K\vec{\boldsymbol{N}}_S||^2 = \frac{\mathrm{d}}{\mathrm{d}t}({}_K\vec{\boldsymbol{N}}_S^{\mathrm{T}}\,{}_K\vec{\boldsymbol{N}}_S) = 2(\boldsymbol{\Theta}\boldsymbol{\omega})^{\mathrm{T}}\boldsymbol{\Theta}\dot{\boldsymbol{\omega}} = -2(\boldsymbol{\Theta}\boldsymbol{\omega})^{\mathrm{T}}\big(\boldsymbol{\omega} \times (\boldsymbol{\Theta}\boldsymbol{\omega})\big) = \mathbf{0}\,. \tag{14}$$

Stationary motion

A rigid body may undergo a stationary motion for which its angular velocity is constant, i.e. $\dot{\boldsymbol{\omega}} = \mathbf{0}$. We will denote such a stationary motion in state-space as $(\boldsymbol{A}_{IK\star}(t), \boldsymbol{\omega}_\star)$. From the Euler equations (5) we infer that stationary motion is only possible if the term $\boldsymbol{\omega} \times (\boldsymbol{\Theta}\boldsymbol{\omega})$ vanishes. Stationary motion therefore implies that $\boldsymbol{\omega}_\star$ is in an eigendirection of $\boldsymbol{\Theta}$, resulting in three stationary directions of motion ${}_K\vec{\boldsymbol{e}}_x^K, {}_K\vec{\boldsymbol{e}}_y^K, {}_K\vec{\boldsymbol{e}}_z^K$. Without loss of generality, let $\boldsymbol{\omega}_\star = \Omega\boldsymbol{e}_\star$, where $\boldsymbol{e}_\star = \boldsymbol{e}_3 = \begin{bmatrix}0 & 0 & 1\end{bmatrix}^{\mathrm{T}}$ agrees with ${}_K\vec{\boldsymbol{e}}_z^K$. The vector $\boldsymbol{e}_\star$ may be complemented by $\boldsymbol{e}_1 = \begin{bmatrix}1 & 0 & 0\end{bmatrix}^{\mathrm{T}}$ and $\boldsymbol{e}_2 = \begin{bmatrix}0 & 1 & 0\end{bmatrix}^{\mathrm{T}}$ to form an orthonormal basis. The evolution of the orientation of the body during stationary motion

$$\boldsymbol{A}_{IK\star}(t) = \boldsymbol{A}_{IK\star}(0)\mathrm{e}^{\tilde{\boldsymbol{\omega}}_\star t} \tag{15}$$

follows from the closed form solution of the matrix differential equation (6). Without loss of generality, we set $\boldsymbol{A}_{IK\star}(0) = \boldsymbol{I}$. From

$${}_I\vec{\boldsymbol{e}}_z^{K\star}(t) = \boldsymbol{A}_{IK\star}(t)\boldsymbol{e}_3 = \mathrm{e}^{\tilde{\boldsymbol{\omega}}_\star t}\boldsymbol{e}_\star = \boldsymbol{e}_\star = {}_I\vec{\boldsymbol{e}}_z^I \tag{16}$$

it follows that $\vec{\boldsymbol{e}}_z^{K\star} = \vec{\boldsymbol{e}}_z^I$ for all t. The stationary motion $(\boldsymbol{A}_{IK\star}(t), \boldsymbol{\omega}_\star)$ itself cannot be stable, irrespective of the principal axis which is considered, because a small error $\Delta\Omega$ in the magnitude of the angular velocity $\boldsymbol{\omega} = (\Omega + \Delta\Omega)\boldsymbol{e}_\star$ will cause $\boldsymbol{A}_{IK}(t)$ to diverge from $\boldsymbol{A}_{IK\star}(t)$. Hence, instead of the stationary motion we need to study the stability of the axis of rotation, or, more precisely, of a manifold in state-space related to that. Hereto, we consider the distance between the axes

of rotation $\vec{\boldsymbol{e}}_z^{K\star} = \vec{\boldsymbol{e}}_z^{I}$ of the stationary motion and $\vec{\boldsymbol{e}}_z^{K}$ of an arbitrary motion, which we express in the K-frame using the quantity

$$\boldsymbol{d}(t) = {}_K\vec{\boldsymbol{e}}_z^{K\star} - {}_K\vec{\boldsymbol{e}}_z^{K} = {}_K\vec{\boldsymbol{e}}_z^{I} - {}_K\vec{\boldsymbol{e}}_z^{K} = \boldsymbol{A}_{KI}(t)\boldsymbol{e}_\star - \boldsymbol{e}_\star. \tag{17}$$

Furthermore, to parametrize the transformation matrix $\boldsymbol{A}_{IK}(t)$, we also introduce the time-dependent quantities

$$\boldsymbol{h}_1(t) = \boldsymbol{A}_{KI}(t)\boldsymbol{e}_1 - \boldsymbol{e}_1, \tag{18}$$

$$\boldsymbol{h}_2(t) = \boldsymbol{A}_{KI}(t)\boldsymbol{e}_2 - \boldsymbol{e}_2. \tag{19}$$

The transformation matrix may therefore be expressed as

$$\begin{aligned} \boldsymbol{A}_{IK}^{\mathrm{T}}(t) &= \boldsymbol{I} + \begin{bmatrix}\boldsymbol{h}_1(t) & \boldsymbol{h}_2(t) & \boldsymbol{d}(t)\end{bmatrix}\begin{bmatrix}\boldsymbol{e}_1 & \boldsymbol{e}_2 & \boldsymbol{e}_\star\end{bmatrix}^{-1} \\ &= \boldsymbol{I} + \begin{bmatrix}\boldsymbol{h}_1(t) & \boldsymbol{h}_2(t) & \boldsymbol{d}(t)\end{bmatrix}. \end{aligned} \tag{20}$$

Furthermore, we introduce the quantity

$$\boldsymbol{\alpha}(t) = \boldsymbol{\omega}(t) - \boldsymbol{\omega}_\star \tag{21}$$

to express the difference in rotation speed, which is being governed by the Euler equations (5)

$$\boldsymbol{\Theta}\dot{\boldsymbol{\alpha}} + (\boldsymbol{\omega}_\star + \boldsymbol{\alpha}) \times (\boldsymbol{\Theta}(\boldsymbol{\omega}_\star + \boldsymbol{\alpha})) = \boldsymbol{0}. \tag{22}$$

Having introduced the quantities $\boldsymbol{d}$ and $\boldsymbol{\alpha}$, we can define the manifold of stationary rotation in a straightforward way

$$\mathcal{M} = \left\{(\boldsymbol{A}_{IK}, \boldsymbol{\omega}) \in \mathrm{SO}(3) \times \mathbb{R}^3 \mid \boldsymbol{d} = \boldsymbol{0}, \boldsymbol{\alpha} = \boldsymbol{0}\right\}. \tag{23}$$

The dynamics of the distance to the axis of stationary rotation is given by

$$\begin{aligned} \dot{\boldsymbol{d}}(t) = \dot{\boldsymbol{A}}_{KI}(t)\boldsymbol{e}_\star &= \left(\boldsymbol{A}_{IK}(t)\tilde{\boldsymbol{\omega}}(t)\right)^{\mathrm{T}}\boldsymbol{e}_\star \\ &= -\tilde{\boldsymbol{\omega}}(t)\boldsymbol{A}_{KI}(t)\boldsymbol{e}_\star \\ &= -\left(\tilde{\boldsymbol{\omega}}_\star + \tilde{\boldsymbol{\alpha}}(t)\right)\left(\boldsymbol{d}(t) + \boldsymbol{e}_\star\right) \\ &= -\tilde{\boldsymbol{\omega}}_\star\boldsymbol{d}(t) - \tilde{\boldsymbol{\alpha}}(t)\left(\boldsymbol{d}(t) + \boldsymbol{e}_\star\right) \end{aligned} \tag{24}$$

being only dependent on $\boldsymbol{d}$ and $\boldsymbol{\alpha}$. It holds that $\dot{\boldsymbol{d}}(t) = \boldsymbol{0}$ if $\boldsymbol{d} = \boldsymbol{\alpha} = \boldsymbol{0}$ and $\dot{\boldsymbol{\alpha}}(t) = \boldsymbol{0}$ if $\boldsymbol{\alpha} = \boldsymbol{0}$. Hence, the manifold $\mathcal{M}$ of stationary rotation is invariant. The differential equations (24) and (22) can be gathered using $\boldsymbol{y}(t) = \begin{pmatrix}\boldsymbol{d}^{\mathrm{T}} & \boldsymbol{\alpha}^{\mathrm{T}}\end{pmatrix}^{\mathrm{T}}$ in the system of ordinary differential equations

$$\dot{\boldsymbol{y}}(t) = \boldsymbol{f}(\boldsymbol{y}(t)), \tag{25}$$

which is time-autonomous. The stability of the axis of rotation now bears down to the stability of the invariant manifold $\mathcal{M}$, i.e. the stability of the equilibrium $\boldsymbol{y}^\star = \boldsymbol{0}$ of system (25). The stability properties of stationary rotation in the 6-dimensional state-space $\boldsymbol{y}$ will be referred as the extended intermediate axis theorem.

Extended intermediate axis theorem

Stability of rotation around the major principal axis

We consider motion in the vicinity of the stationary rotation $\boldsymbol{\omega}_\star = \Omega\boldsymbol{e}_\star$, $\Omega > 0$, and $C \geq \max(A, B)$ such that $\boldsymbol{e}_\star$ is the major principal axis of inertia. Herein, the $K\star$-frame is the body fixed frame of stationary motion, whereas we will reserve the K-frame for the body fixed frame of an arbitrary motion in the vicinity of the stationary motion. The frames are related through $\boldsymbol{A}_{KK\star} = \boldsymbol{A}_{KI}\boldsymbol{A}_{IK\star} = \boldsymbol{A}_{IK}^{\mathrm{T}}\boldsymbol{A}_{IK\star}$ and it therefore holds that

$$\boldsymbol{A}_{KK\star}\boldsymbol{e}_\star = \boldsymbol{A}_{KI}\boldsymbol{A}_{IK\star}\boldsymbol{e}_\star = \boldsymbol{A}_{KI}\boldsymbol{e}_\star = \boldsymbol{d} + \boldsymbol{e}_\star. \tag{26}$$

In order to set up a Lyapunov function, we consider the function

$$\bar{V}(\boldsymbol{d}, \boldsymbol{\alpha}) = \|{}_I\vec{\boldsymbol{N}}_S - {}_I\vec{\boldsymbol{N}}_{S\star}\|^2 = \|{}_K\vec{\boldsymbol{N}}_S - {}_K\vec{\boldsymbol{N}}_{S\star}\|^2. \tag{27}$$

The spin $\vec{\boldsymbol{N}}_{S\star}$ can be easily expressed in the $K\star$-frame as ${}_{K\star}\vec{\boldsymbol{N}}_{S\star} = \boldsymbol{\Theta}\boldsymbol{\omega}_\star = C\Omega\boldsymbol{e}_\star$, which can be cast in the K-frame through

$${}_K\vec{\boldsymbol{N}}_{S\star} = \boldsymbol{A}_{KK\star}\,{}_{K\star}\vec{\boldsymbol{N}}_{S\star} = C\Omega\,\boldsymbol{A}_{KK\star}\boldsymbol{e}_\star = C\Omega(\boldsymbol{d} + \boldsymbol{e}_\star). \tag{28}$$

Using ${}_K\vec{\boldsymbol{N}}_S = \boldsymbol{\Theta}\boldsymbol{\omega} = \boldsymbol{\Theta}(\boldsymbol{\alpha} + \boldsymbol{\omega}_\star) = \boldsymbol{\Theta}\boldsymbol{\alpha} + C\Omega\boldsymbol{e}_\star$ we arrive at

$$\bar{V}(\boldsymbol{d}, \boldsymbol{\alpha}) = \|\boldsymbol{\Theta}\boldsymbol{\alpha} - C\Omega\boldsymbol{d}\|^2 = (A\alpha_x - C\Omega d_x)^2 + (B\alpha_y - C\Omega d_y)^2 + (C\alpha_z - C\Omega d_z)^2. \tag{29}$$

Furthermore, we introduce the function

$$\hat{V}(\boldsymbol{\alpha}) = 2C\,T(\boldsymbol{\omega}) - \|\vec{\boldsymbol{N}}_S(\boldsymbol{\omega})\|^2 + \frac{1}{\Omega^2}(2\,T(\boldsymbol{\omega}) - 2\,T(\boldsymbol{\omega}_\star))^2\,, \tag{30}$$

which can be expressed as

$$\begin{aligned}\hat{V}(\boldsymbol{\alpha}) &= C\boldsymbol{\omega}^{\mathrm{T}}\boldsymbol{\Theta}\boldsymbol{\omega} - \boldsymbol{\omega}^{\mathrm{T}}\boldsymbol{\Theta}^2\boldsymbol{\omega} + \frac{1}{\Omega^2}(\boldsymbol{\omega}^{\mathrm{T}}\boldsymbol{\Theta}\boldsymbol{\omega} - \boldsymbol{\omega}_\star^{\mathrm{T}}\boldsymbol{\Theta}\boldsymbol{\omega}_\star)^2 \\ &= (\boldsymbol{\alpha}+\boldsymbol{\omega}_\star)^{\mathrm{T}}(C\boldsymbol{\Theta}-\boldsymbol{\Theta}^2)(\boldsymbol{\alpha}+\boldsymbol{\omega}_\star) + \frac{1}{\Omega^2}\left((\boldsymbol{\alpha}+\boldsymbol{\omega}_\star)^{\mathrm{T}}\boldsymbol{\Theta}(\boldsymbol{\alpha}+\boldsymbol{\omega}_\star) - \boldsymbol{\omega}_\star^{\mathrm{T}}\boldsymbol{\Theta}\boldsymbol{\omega}_\star\right)^2 \\ &= \boldsymbol{\alpha}^{\mathrm{T}}(C\boldsymbol{\Theta}-\boldsymbol{\Theta}^2)\boldsymbol{\alpha} + \frac{1}{\Omega^2}\left(\boldsymbol{\alpha}^{\mathrm{T}}\boldsymbol{\Theta}\boldsymbol{\alpha} + 2C\boldsymbol{\omega}_\star^{\mathrm{T}}\boldsymbol{\alpha}\right)^2 \\ &= A(C-A)\alpha_x^2 + B(C-B)\alpha_y^2 + \frac{1}{\Omega^2}(A\alpha_x^2 + B\alpha_y^2 + C\alpha_z^2 + 2C\Omega\alpha_z)^2\end{aligned} \tag{31}$$

To prove stability of the trivial equilibrium of (25) for $C \geq \max(A,B)$, we consider the Lyapunov candidate function

$$V(\boldsymbol{y}) = \bar{V}(\boldsymbol{d},\boldsymbol{\alpha}) + \hat{V}(\boldsymbol{\alpha}), \tag{32}$$

which purely consists of the invariants of motion $\vec{\boldsymbol{N}}_S = \text{const.}$ and $T(\boldsymbol{\omega}) = \text{const.}$ and is therefore constant, i.e. $\dot{V} = 0$ along solutions of the system. The (local) positive definiteness of V remains to be investigated in the following.
First, we show that $\hat{V}(\boldsymbol{\alpha})$ is a local positive definite function in $\boldsymbol{\alpha}$. We infer that $\hat{V}(\boldsymbol{\alpha}) \geq 0$ for arbitrary $\boldsymbol{\alpha} \in \mathbb{R}^3$ as it is a sum of squares with positive coefficients for $C \geq \max(A,B)$. Moreover, the points where $\hat{V}(\boldsymbol{\alpha}) = 0$ are characterized by $\alpha_x = 0$, $\alpha_y = 0$ and $\alpha_z(\alpha_z + 2\Omega) = 0$. This implies that $\hat{V}$ vanishes at the origin and at the point $\boldsymbol{\alpha} = (0\ 0\ -2\Omega)^{\mathrm{T}}$ and is strictly positive for all other $\boldsymbol{\alpha} \in \mathbb{R}^3$, proving that $\hat{V}(\boldsymbol{\alpha})$ is locally positive definite.
As V is the sum of $\bar{V}(\boldsymbol{d},\boldsymbol{\alpha}) \geq 0$ and $\hat{V}(\boldsymbol{\alpha}) \geq 0$, it may only vanish if $\bar{V}(\boldsymbol{d},\boldsymbol{\alpha})$ and $\hat{V}(\boldsymbol{\alpha})$ vanish simultaneously. From the local positive definiteness of $\hat{V}(\boldsymbol{\alpha})$ it is clear that, in the neighborhood of the origin, V may only vanish for $\boldsymbol{\alpha} = \boldsymbol{0}$. Now we consider $\bar{V}(\boldsymbol{d},\boldsymbol{\alpha})$ and note that $\bar{V}(\boldsymbol{d},\boldsymbol{0}) = C^2\Omega^2\|\boldsymbol{d}\|^2$ can only vanish if $\boldsymbol{d} = \boldsymbol{0}$. This proves local positive definiteness of V and, thereby, that rotation around the major principal axis is stable. This result may be viewed as an *extended* intermediate axis theorem, as it not only proves that the angular velocity $\boldsymbol{\omega}$ remains close to $\boldsymbol{\omega}_\star$ (i.e. the classical intermediate axis theorem), but also proves that $\boldsymbol{d}$ remains small, i.e. the orientation of the axis of rotation is stable.

Stability of rotation around the minor principal axis

We now consider the stability of stationary rotation around the minor principal axis by setting again $\boldsymbol{\omega}_\star = \Omega\boldsymbol{e}_\star$, $\Omega > 0$ with $\boldsymbol{e}_\star = \boldsymbol{e}_3$ but assuming $C \leq \min(A,B)$. The proof of the stability of stationary rotation around the minor principal axis is completely analogous to the proof for the major principal axis.
We consider again the Lyapunov candidate function of the form

$$V(\boldsymbol{y}) = \bar{V}(\boldsymbol{d},\boldsymbol{\alpha}) + \hat{V}(\boldsymbol{\alpha}), \tag{33}$$

where the function

$$\bar{V}(\boldsymbol{d},\boldsymbol{\alpha}) = \|\boldsymbol{\Theta}\boldsymbol{\alpha} - C\Omega\boldsymbol{d}\|^2 = (A\alpha_x - C\Omega d_x)^2 + (B\alpha_y - C\Omega d_y)^2 + (C\alpha_z - C\Omega d_z)^2 \tag{34}$$

is defined as before, but $\hat{V}(\boldsymbol{\alpha})$ is chosen as

$$\begin{aligned}\hat{V}(\boldsymbol{\alpha}) &= -C\boldsymbol{\omega}^{\mathrm{T}}\boldsymbol{\Theta}\boldsymbol{\omega} + \boldsymbol{\omega}^{\mathrm{T}}\boldsymbol{\Theta}^2\boldsymbol{\omega} + \frac{1}{\Omega^2}(\boldsymbol{\omega}^{\mathrm{T}}\boldsymbol{\Theta}\boldsymbol{\omega} - \boldsymbol{\omega}_\star^{\mathrm{T}}\boldsymbol{\Theta}\boldsymbol{\omega}_\star)^2 \\ &= A(A-C)\alpha_x^2 + B(B-C)\alpha_y^2 + \frac{1}{\Omega^2}(A\alpha_x^2 + B\alpha_y^2 + C\alpha_z^2 + 2C\Omega\alpha_z)^2\end{aligned} \tag{35}$$

The Lyapunov function is constant along solutions and is locally positive definite for $C \leq \min(A,B)$, proving stability of rotation around the minor principal axis.

Fully explicit scheme

We briefly discuss the fully explicit scheme (or pseudo-implicit scheme) which is currently implemented in RAMMS:rockfall. Let $\boldsymbol{\omega}^k$ denote the angular velocity of the rock at time instant t^k. The present scheme calculates the angular velocity $\boldsymbol{\omega}^{k+1}$ at time instant $t^{k+1} = t^k + \Delta t$ (in the absence of contact with the terrain) through

$$\boldsymbol{\Theta}(\boldsymbol{\omega}^{k+1} - \boldsymbol{\omega}^k) + \frac{\Delta t}{2}\boldsymbol{G}(\boldsymbol{\omega}^k)(\boldsymbol{\omega}^{k+1} + \boldsymbol{\omega}^k) = 0\ , \tag{36}$$

where $\boldsymbol{G}(\boldsymbol{\omega}) = \boldsymbol{\Theta}\tilde{\boldsymbol{\omega}} + \tilde{\boldsymbol{\omega}}\boldsymbol{\Theta}$, resulting the explicit velocity update

$$\boldsymbol{\omega}^{k+1} = \left(\boldsymbol{\Theta} + \frac{\Delta t}{2}\boldsymbol{G}(\boldsymbol{\omega}^k)\right)^{-1}\left(\boldsymbol{\Theta} - \frac{\Delta t}{2}\boldsymbol{G}(\boldsymbol{\omega}^k)\right)\boldsymbol{\omega}^k = \boldsymbol{\omega}^k - \left(\boldsymbol{\Theta} + \frac{\Delta t}{2}\boldsymbol{G}(\boldsymbol{\omega}^k)\right)^{-1}\boldsymbol{G}(\boldsymbol{\omega}^k)\boldsymbol{\omega}^k, \tag{37}$$

where the last step is a simplification explained in [5]. The rotation matrix is parametrized using a quaternion $\boldsymbol{q}^k$ with a midpoint update rule

$$\boldsymbol{q}_{\text{pre}}^{k+1} = \boldsymbol{q}^{k+\frac{1}{2}} + \frac{\Delta t}{2}\boldsymbol{F}(\boldsymbol{q}^{k+\frac{1}{2}})\boldsymbol{\omega}^{k+1}, \qquad \boldsymbol{q}^{k+1} = \frac{\boldsymbol{q}_{\text{pre}}^{k+1}}{\|\boldsymbol{q}_{\text{pre}}^{k+1}\|}, \tag{38}$$

where $\boldsymbol{q}^{k+\frac{1}{2}} = \boldsymbol{q}^k + \frac{\Delta t}{2}\boldsymbol{\omega}^k$.
The rationale behind the explicit scheme is that it preserves the kinetic energy. The change in kinetic energy over the time step is

$$\begin{aligned} T(\boldsymbol{\omega}^{k+1}) - T(\boldsymbol{\omega}^k) &= \frac{1}{2}(\boldsymbol{\omega}^{k+1})^{\mathrm{T}}\boldsymbol{\Theta}\boldsymbol{\omega}^{k+1} - \frac{1}{2}(\boldsymbol{\omega}^k)^{\mathrm{T}}\boldsymbol{\Theta}\boldsymbol{\omega}^k \\ &= \frac{1}{2}(\boldsymbol{\omega}^{k+1} + \boldsymbol{\omega}^k)^{\mathrm{T}}\boldsymbol{\Theta}(\boldsymbol{\omega}^{k+1} - \boldsymbol{\omega}^k). \end{aligned} \tag{39}$$

Substitution of the explicit scheme (36) yields

$$T(\boldsymbol{\omega}^{k+1}) - T(\boldsymbol{\omega}^k) = -\frac{\Delta t}{4}(\boldsymbol{\omega}^{k+1} + \boldsymbol{\omega}^k)^{\mathrm{T}}\boldsymbol{G}(\boldsymbol{\omega}^k)(\boldsymbol{\omega}^{k+1} + \boldsymbol{\omega}^k) = 0 \tag{40}$$

due to the skew-symmetry of $\boldsymbol{G}(\boldsymbol{\omega})$ which shows that the kinetic energy is conserved. A stationary solution $\boldsymbol{\omega}_\star = \boldsymbol{\omega}^k = \boldsymbol{\omega}^{k+1}$ of the scheme respects

$$\boldsymbol{G}(\boldsymbol{\omega}_\star)\boldsymbol{\omega}_\star = \boldsymbol{\omega}_\star \times (\boldsymbol{\Theta}\boldsymbol{\omega}_\star) = 0\ , \tag{41}$$

and corresponds to a stationary rotation of the Euler equations around principal axes.
Let $\boldsymbol{\alpha}^k$ be the perturbation of the angular velocity with respect to the stationary rotation $\boldsymbol{\omega}_\star = \Omega \boldsymbol{e}_\star$ around the principal axis $\boldsymbol{e}_\star = \boldsymbol{e}_3$. The perturbation dynamics is obtained using $\boldsymbol{\omega}^k = \boldsymbol{\omega}_\star + \boldsymbol{\alpha}^k$ as

$$\boldsymbol{\Theta}(\boldsymbol{\alpha}^{k+1} - \boldsymbol{\alpha}^k) + \frac{\Delta t}{2}\boldsymbol{G}(\boldsymbol{\omega}_\star)(\boldsymbol{\alpha}^{k+1} + \boldsymbol{\alpha}^k) + \frac{\Delta t}{2}\boldsymbol{G}(\boldsymbol{\alpha}^k)(\boldsymbol{\alpha}^{k+1} + \boldsymbol{\alpha}^k) + \Delta t\boldsymbol{G}(\boldsymbol{\alpha}^k)\boldsymbol{\omega}_\star = 0\ , \tag{42}$$

where the linearity of $\boldsymbol{G}$ and (41) have been used. For small perturbations we can neglect higher order terms in $\boldsymbol{\alpha}^k$ giving the linearized perturbation dynamics

$$\begin{aligned} \boldsymbol{0} &= \boldsymbol{\Theta}(\boldsymbol{\alpha}^{k+1} - \boldsymbol{\alpha}^k) + \frac{\Delta t}{2}\boldsymbol{G}(\boldsymbol{\omega}_\star)(\boldsymbol{\alpha}^{k+1} + \boldsymbol{\alpha}^k) + \Delta t\boldsymbol{G}(\boldsymbol{\alpha}^k)\boldsymbol{\omega}_\star \\ &= \left[\boldsymbol{\Theta} + \frac{\Delta t}{2}\boldsymbol{G}(\boldsymbol{\omega}_\star)\right](\boldsymbol{\alpha}^{k+1} - \boldsymbol{\alpha}^k) + \Delta t\big(\boldsymbol{G}(\boldsymbol{\alpha}^k)\boldsymbol{\omega}_\star + \boldsymbol{G}(\boldsymbol{\omega}_\star)\boldsymbol{\alpha}^k\big)\ . \end{aligned} \tag{43}$$

The linearized perturbation dynamics can be solved for $\boldsymbol{\alpha}^{k+1}$ explicitly. Hereto, the second term is reformulated as

$$\begin{aligned} \boldsymbol{G}(\boldsymbol{\alpha}^k)\boldsymbol{\omega}_\star + \boldsymbol{G}(\boldsymbol{\omega}_\star)\boldsymbol{\alpha}^k &= \boldsymbol{\Theta}\tilde{\boldsymbol{\alpha}}^k\boldsymbol{\omega}_\star + \tilde{\boldsymbol{\alpha}}^k\boldsymbol{\Theta}\boldsymbol{\omega}_\star + \boldsymbol{\Theta}\tilde{\boldsymbol{\omega}}_\star\boldsymbol{\alpha}^k + \tilde{\boldsymbol{\omega}}_\star\boldsymbol{\Theta}\boldsymbol{\alpha}^k \\ &= \tilde{\boldsymbol{\alpha}}^k\boldsymbol{\Theta}\boldsymbol{\omega}_\star + \tilde{\boldsymbol{\omega}}_\star\boldsymbol{\Theta}\boldsymbol{\alpha}^k \\ &= \boldsymbol{\alpha}^k \times (\boldsymbol{\Theta}\boldsymbol{\omega}_\star) + \boldsymbol{\omega}_\star \times (\boldsymbol{\Theta}\boldsymbol{\alpha}^k) \\ &=: \boldsymbol{A}\boldsymbol{\alpha}^k\ , \end{aligned} \tag{44}$$

where $\boldsymbol{A} = -\widetilde{(\boldsymbol{\Theta}\boldsymbol{\omega}_\star)} + \tilde{\boldsymbol{\omega}}_\star\boldsymbol{\Theta}$. Next, the matrix $\boldsymbol{B} = \boldsymbol{\Theta} + \frac{\Delta t}{2}\boldsymbol{G}(\boldsymbol{\omega}_\star)$ in (43) has the inverse

$$\boldsymbol{B}^{-1} = \frac{1}{\det \boldsymbol{B}}\begin{pmatrix} BC & \frac{\Delta t}{2}\Omega C(A+B) & 0 \\ -\frac{\Delta t}{2}\Omega C(A+B) & AC & 0 \\ 0 & 0 & \frac{\det \boldsymbol{B}}{C} \end{pmatrix}\ , \tag{45}$$

where the determinant of $\boldsymbol{B}$ is given by $\det \boldsymbol{B} = ABC + \frac{\Delta t^2}{4}C(A+B)^2$. Hence, the linearized perturbation dynamics can be given in the explicit form

$$\boldsymbol{\alpha}^{k+1} = \left(\boldsymbol{I} - \Delta t\boldsymbol{B}^{-1}\boldsymbol{A}\right)\boldsymbol{\alpha}^k = \boldsymbol{D}\boldsymbol{\alpha}^k\ , \tag{46}$$

in which the matrix $\boldsymbol{D}$ has the non-zero components

$$\begin{aligned} &D_{11} = 1 - \frac{\Delta t^2}{2\det \boldsymbol{B}}\Omega^2 C(A+B)(A-C), \quad D_{12} = -\frac{\Delta t}{\det \boldsymbol{B}}\Omega AC(A-C), \\ &D_{21} = -\frac{\Delta t}{\det \boldsymbol{B}}\Omega BC(C-B) \qquad\qquad D_{22}, = 1 + \frac{\Delta t^2}{2\det \boldsymbol{B}}\Omega^2 C(A+B)(C-B), \\ &D_{33} = 1. \end{aligned} \tag{47}$$

The stability of rotation around the major principal axis is determined through the eigenvalues of $\boldsymbol{D}$, being the roots of the characteristic polynomial

$$\begin{aligned}\det(\lambda\boldsymbol{I}-\boldsymbol{D}) &= (\lambda-1)\left[(\lambda-D_{11})(\lambda-D_{22})-D_{12}D_{21})\right] \\ &= (\lambda-1)\left[\lambda^2-(D_{11}+D_{22})\lambda+(D_{11}D_{22}-D_{12}D_{21})\right]\end{aligned} \tag{48}$$

given by

$$\lambda_{1/2}=\frac{b\pm\sqrt{b^2-4c}}{2} \quad \text{and} \quad \lambda_3=1. \tag{49}$$

Herein, the parameters $b=D_{11}+D_{22}$ and $c=D_{11}D_{22}-D_{12}D_{21}$ can be calculated as

$$b=2-\frac{\Delta t^2\Omega^2}{2\det\boldsymbol{B}}C(A+B)(A+B-2C), \quad c=1+\frac{\Delta t^2\Omega^2}{2\det\boldsymbol{B}}C\left((A+B)\left(A+B-2C\right)-2\left(A-C\right)\left(C-B\right)\right)\ .$$

The eigenvalues $\lambda_{1/2}$ in (49) take the form

$$\lambda_{1/2}=1-\frac{d}{2}\pm\frac{\sqrt{d^2+4e}}{2} \tag{50}$$

with

$$d=\frac{\Delta t^2}{2\det\boldsymbol{B}}\Omega^2C(A+B)(A+B-2C), \qquad e=\frac{\Delta t^2}{\det\boldsymbol{B}}\Omega^2C(A-C)(C-B) \tag{51}$$

For rotation around the major principal axis it holds that $C\geq\max(A,B)$ from which follows that $d<0$. Therefore, at least one of the eigenvalues has a magnitude larger than unity which proves instability of rotation around the major principal axis, contrary to the intermediate axis theorem. Hence, the explicit scheme cannot correctly represent the stability properties of a freely rotating body.

A stability preserving implicit scheme

Here, we propose an alternative scheme for rockfall simulation with RAMMS:rockfall which preserves the stability properties of the principal axes of rotation in accordance with the intermediate axis theorem. The alternative scheme consists of two parts:

1. as update rule for the angular velocity, we use the implicit scheme proposed by [5]
2. as update rule for the orientation parametrization, we propose a novel scheme which preserves the spin.

The implicit scheme for the angular velocity calculates $\boldsymbol{\omega}^{k+1}$ at time instant $t^{k+1}=t^k+\Delta t$ during a flight phase as

$$\boldsymbol{\Theta}(\boldsymbol{\omega}^{k+1}-\boldsymbol{\omega}^k)+\Delta t\boldsymbol{\omega}^{k+\frac{1}{2}}\times(\boldsymbol{\Theta}\boldsymbol{\omega}^{k+\frac{1}{2}})=0 \quad \text{with} \quad \boldsymbol{\omega}^{k+\frac{1}{2}}=\frac{1}{2}(\boldsymbol{\omega}^k+\boldsymbol{\omega}^{k+1})\ . \tag{52}$$

Substitution of the scheme (52) in the kinetic energy expression (39) yields

$$T(\boldsymbol{\omega}^{k+1})-T(\boldsymbol{\omega}^k)=-\frac{\Delta t}{2}(\boldsymbol{\omega}^{k+\frac{1}{2}})^{\mathrm{T}}\left[\boldsymbol{\omega}^{k+\frac{1}{2}}\times(\boldsymbol{\Theta}\boldsymbol{\omega}^{k+\frac{1}{2}})\right]=0\ . \tag{53}$$

showing that the kinetic energy is preserved by the implicit scheme. The magnitude of the spin $\|\vec{\boldsymbol{N}}_S\|=\|_K\vec{\boldsymbol{N}}_S\|=\|\boldsymbol{\Theta}\boldsymbol{\omega}\|$, defined by (12), is only dependent on the angular velocity. The implicit scheme for the angular velocity also conserves the magnitude of the spin as follows from

$$\begin{aligned}||\vec{\boldsymbol{N}}_S^{k+1}||^2-||\vec{\boldsymbol{N}}_S^{k}||^2 &= (\boldsymbol{\Theta}\boldsymbol{\omega}^{k+1})^{\mathrm{T}}\boldsymbol{\Theta}\boldsymbol{\omega}^{k+1}-(\boldsymbol{\Theta}\boldsymbol{\omega}^{k})^{\mathrm{T}}\boldsymbol{\Theta}\boldsymbol{\omega}^{k} \\ &= (\boldsymbol{\Theta}\boldsymbol{\omega}^{k+\frac{1}{2}})^{\mathrm{T}}\boldsymbol{\Theta}(\boldsymbol{\omega}^{k+1}-\boldsymbol{\omega}^{k}) \\ &\overset{(52)}{=} -\Delta t(\boldsymbol{\Theta}\boldsymbol{\omega}^{k+\frac{1}{2}})^{\mathrm{T}}\left[\boldsymbol{\omega}^{k+\frac{1}{2}}\times(\boldsymbol{\Theta}\boldsymbol{\omega}^{k+\frac{1}{2}})\right]=0\ .\end{aligned} \tag{54}$$

We now propose an update rule for the orientation parametrization. The update of the orientation $\boldsymbol{A}_{IK}^{k+1}$ is chosen such that the spin remains constant, i.e.

$${}_I\vec{\boldsymbol{N}}_S^{k+1}={}_I\vec{\boldsymbol{N}}_S^{k}, \tag{55}$$

and such that the kinematic equation is correctly approximated in the sense that

$$\lim_{\Delta t\downarrow 0}\frac{\boldsymbol{A}_{IK}^{k+1}-\boldsymbol{A}_{IK}^{k}}{\Delta t}=\dot{\boldsymbol{A}}_{IK}(t^k) \tag{56}$$

where $\dot{\boldsymbol{A}}_{IK} = \boldsymbol{A}_{IK}(t)\tilde{\boldsymbol{\omega}}$. We choose an update of the form

$$\boldsymbol{A}_{IK}^{k+1} = \boldsymbol{A}_{IK}^{k} \mathrm{e}^{\tilde{\boldsymbol{\omega}}^{k+\frac{1}{2}}\Delta t} \boldsymbol{B}(\boldsymbol{\omega}^k, \boldsymbol{\omega}^{k+1}) \tag{57}$$

where the matrix $\boldsymbol{B}$ depends on $\boldsymbol{\omega}^k$ and $\boldsymbol{\omega}^{k+1}$ and needs to fulfill $\boldsymbol{B}^{\mathrm{T}}\boldsymbol{B} = \boldsymbol{I}$ to ensure that $(\boldsymbol{A}_{IK}^{k+1})^{\mathrm{T}}\boldsymbol{A}_{IK}^{k+1} = \boldsymbol{I}$. Furthermore, we demand that $\boldsymbol{B}(\boldsymbol{x}, \boldsymbol{x}) = \boldsymbol{I}$ for all $\boldsymbol{x}$ such that

$$\lim_{\Delta t \downarrow 0} \boldsymbol{B}(\boldsymbol{\omega}^k, \boldsymbol{\omega}^{k+1}) = \boldsymbol{B}(\boldsymbol{\omega}^k, \boldsymbol{\omega}^k) = \boldsymbol{I} \tag{58}$$

from which follows the kinematic consistency (56).
To ensure the conservation of spin we demand

$$\boldsymbol{A}_{IK}^{k+1}\boldsymbol{\Theta}\boldsymbol{\omega}^{k+1} = \boldsymbol{A}_{IK}^{k}\boldsymbol{\Theta}\boldsymbol{\omega}^{k} \tag{59}$$

which, after substitution of the update rule, gives

$$\boldsymbol{A}_{IK}^{k} \mathrm{e}^{\tilde{\boldsymbol{\omega}}^{k+\frac{1}{2}}\Delta t} \boldsymbol{B}(\boldsymbol{\omega}^k, \boldsymbol{\omega}^{k+1})\boldsymbol{\Theta}\boldsymbol{\omega}^{k+1} = \boldsymbol{A}_{IK}^{k}\boldsymbol{\Theta}\boldsymbol{\omega}^{k}. \tag{60}$$

The matrix $\boldsymbol{B}$ will now be chosen such that

$$\mathrm{e}^{\tilde{\boldsymbol{\omega}}^{k+\frac{1}{2}}\Delta t} \boldsymbol{B}(\boldsymbol{\omega}^k, \boldsymbol{\omega}^{k+1})\boldsymbol{\Theta}\boldsymbol{\omega}^{k+1} = \boldsymbol{\Theta}\boldsymbol{\omega}^{k} \tag{61}$$

and therefore

$$\boldsymbol{B}(\boldsymbol{\omega}^k, \boldsymbol{\omega}^{k+1})\boldsymbol{\Theta}\boldsymbol{\omega}^{k+1} = \mathrm{e}^{-\tilde{\boldsymbol{\omega}}^{k+\frac{1}{2}}\Delta t}\boldsymbol{\Theta}\boldsymbol{\omega}^{k} \tag{62}$$

from which we see that it is indeed only dependent on $\boldsymbol{\omega}^k$ and $\boldsymbol{\omega}^{k+1}$. The matrix $\boldsymbol{B}$ is a pure rotation.
Using Rodrigues formula, every pure rotation $\boldsymbol{R}$ around the unit vector $\boldsymbol{k}$ with rotation angle θ can be represented as

$$\boldsymbol{R} = \boldsymbol{I} + \sin\theta\boldsymbol{K} + (1 - \cos\theta)\boldsymbol{K}^2 \tag{63}$$

where $\boldsymbol{K} = \tilde{\boldsymbol{k}}$. If $\boldsymbol{k}$ and θ are chosen as

$$\boldsymbol{k} = \frac{\boldsymbol{b} \times \boldsymbol{c}}{\|\boldsymbol{b} \times \boldsymbol{c}\|}, \quad \cos\theta = \frac{\boldsymbol{b} \cdot \boldsymbol{c}}{\|\boldsymbol{b}\|\|\boldsymbol{c}\|} \tag{64}$$

then it holds that $\boldsymbol{R}\boldsymbol{b} = \boldsymbol{c}$ if $\|\boldsymbol{b}\| = \|\boldsymbol{c}\|$. Furthermore, it holds that $\boldsymbol{R} \to \boldsymbol{I}$ for $\boldsymbol{b} \to \boldsymbol{c}$.
Hence, we choose $\boldsymbol{B} = \boldsymbol{I} + \sin\theta\boldsymbol{K} + (1 - \cos\theta)\boldsymbol{K}^2$ with

$$\boldsymbol{k} = \frac{\boldsymbol{\Theta}\boldsymbol{\omega}^{k+1} \times (\mathrm{e}^{-\tilde{\boldsymbol{\omega}}^{k+\frac{1}{2}}\Delta t}\boldsymbol{\Theta}\boldsymbol{\omega}^{k})}{\|\boldsymbol{\Theta}\boldsymbol{\omega}^{k+1} \times (\mathrm{e}^{-\tilde{\boldsymbol{\omega}}^{k+\frac{1}{2}}\Delta t}\boldsymbol{\Theta}\boldsymbol{\omega}^{k})\|}, \quad \cos\theta = \frac{\boldsymbol{\Theta}\boldsymbol{\omega}^{k+1} \cdot (\mathrm{e}^{-\tilde{\boldsymbol{\omega}}^{k+\frac{1}{2}}\Delta t}\boldsymbol{\Theta}\boldsymbol{\omega}^{k})}{\|\boldsymbol{\Theta}\boldsymbol{\omega}^{k+1}\|\|\boldsymbol{\Theta}\boldsymbol{\omega}^{k}\|}. \tag{65}$$

To prove that the proposed scheme has the desired stability properties of the principal axes of rotation, we use the Lyapunov functions $V(\boldsymbol{y}^k)$ for the major and minor principal axes as presented before. As the proposed scheme conserves the kinetic energy and the spin by construction it holds that $V(\boldsymbol{y}^{k+1}) = V(\boldsymbol{y}^k)$, whereas positive definiteness has already been shown. The proposed scheme therefore preserves the stability properties of the principal axes of rotation in accordance with the extended intermediate axis theorem.

Numerical results

We compare the explicit and the implicit scheme on a numerical example. We consider a cuboid of mass $m = 1$ kg with length $a = 3$ m, width $b = 2$ m and height $c = 1$ m in the $\vec{\boldsymbol{e}}_x^K$, $\vec{\boldsymbol{e}}_y^K$ and $\vec{\boldsymbol{e}}_z^K$) direction, respectively. The principal moments of inertia are therefore $A = \frac{m}{12}(b^2 + c^2)$, $B = \frac{m}{12}(a^2 + c^2)$ and $C = \frac{m}{12}(a^2 + b^2)$ such that $A < B < C$. Rotation in the neighborhood of stationary rotation $\boldsymbol{\omega}_\star = \Omega\boldsymbol{e}_\star$ around the major principal axis $\boldsymbol{e}_\star = \boldsymbol{e}_3$ is considered. As initial conditions we choose $\boldsymbol{A}_{IK}(0) = \boldsymbol{I}$ and $\boldsymbol{\omega} = \begin{pmatrix}\omega_x & \omega_y & \omega_z\end{pmatrix}^{\mathrm{T}} = \begin{pmatrix}10^{-3} & 10^{-3} & 10\end{pmatrix}^{\mathrm{T}}$ rad/s. We simulate 20 s using a time-step of $\Delta t = 0.01$ s using the explicit and implicit scheme. The results of both schemes are shown in Figures 1 and 2. The body initially rotates in the vicinity of the major principal axis with angular velocity $\omega_z = \Omega = 10$ rad/s, which is stable as follows from the extended intermediate axis theorem. However, in the numerical solution of the explicit scheme, the body deviates from stationary rotation around the major principal axis (approximately at $t = 10$ s) and tends to stable rotation around the minor principal axis with angular speed $\omega_x = -\sqrt{\frac{C}{A}}\Omega$. If a smaller time-step is taken in the explicit scheme, then the change of axis will be slower and will take place at a later point in time. The solution of the implicit scheme remains very close to the major principal axis, both in angular velocity and in the distance $\boldsymbol{d}(t) = {}_K\vec{\boldsymbol{e}}_z^{K\star} - {}_K\vec{\boldsymbol{e}}_z^K$ and is therefore much more accurate.

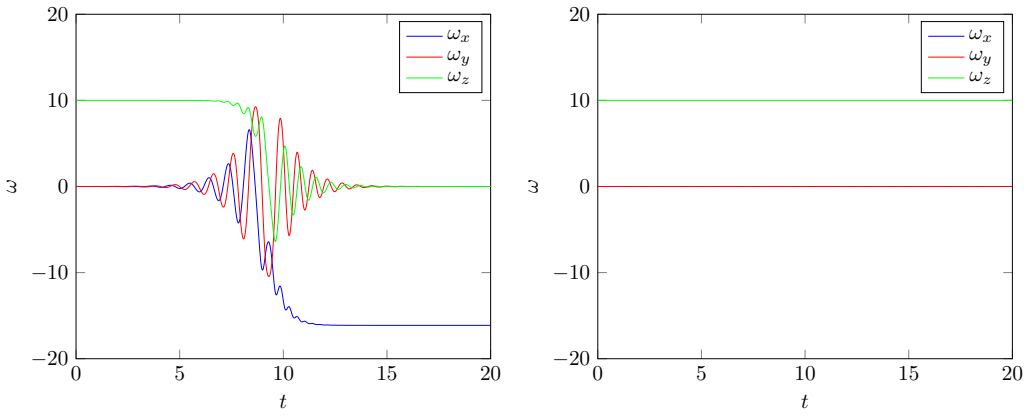

Figure 1: Angular velocities: left the explicit scheme, right the implicit scheme

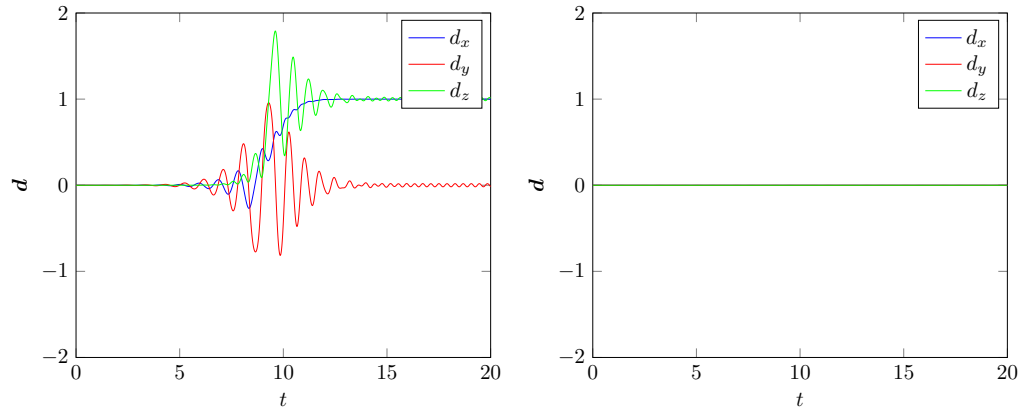

Figure 2: Distance $\boldsymbol{d}(t) = {}_K\vec{e}_z^{K\star} - {}_K\vec{e}_z^{K}$: left the explicit scheme, right the implicit scheme

Simulation results with RAMMS::ROCKFALL

In rockfall events the rotation of platy disk-shaped rocks around their major principal axis is a remarkable phenomenon which has been recently precisely measured in experiments [1]. In order to capture these rock dynamics, we have fully implemented the newly proposed implicit scheme into RAMMS::ROCKFALL and have performed simulations in both idealized and actual rockfall environments. As a control group, the original explicit scheme employed in the current RAMMS:ROCKFALL version has been utilized to obtain rockfall simulations under the same boundary conditions.
The first group of simulations was performed with a disk-shaped rock going downward an idealized inclined slope of 40°. The rock has a uniformly distributed mass of 1000 kg and has a geometry size of 1.16, 1.14 and 0.35 m along its three principal axes, respectively (see Tab. 3). In total 300 simulations were performed with only changing the initial rock orientation. The same initial rock orientation set and time step (0.002 s) was employed for both the explicit and the implicit scheme [4]. Fig. 3 compares for both numerical schemes the kinetic rock energy using the statistic mode of RAMMS::ROCKFALL (first row). The trajectory mode (second row) shows for a single simulation the development of rock rotations along its principal axes. The implicit scheme tends to give significantly lower and much more homogeneous values of the kinetic energy. Furthermore, it takes a much shorter distance for rocks calculated with the implicit scheme to enter the mode rotating around their major principal axes, which remains stable until the rock reaches the horizontal deposition zone. Tab. 1 compares the corresponding mean and standard deviation values obtained for the both numerical schemes. The second group of simulations was performed with a so-called EOTA-shaped rock (see Tab. 3) which was used in rockfall experiments with instrumented rocks at Chant Sura in Davos, Switzerland [1]. The rock mass is 780 kg, homogeneously distributed in a rigid body of 0.93, 0.93 and 0.47 m along the three principal axes. Also 300 simulations

Table 1: Comparison of 300 rocks behavior on an idealized slope for the explicit and the implicit schemes.

Parameter	**Explicit**		**Implicit**	
	Mean	Standard Deviation	Mean	Standard Deviation
kinetic energy (kJ)	127.95	107.25	78.13	43.08
translational velocity (m/s)	13.35	6.29	10.59	3.48
rotational velocity (rot/s)	3.01	1.39	2.47	0.77
jump height (m)	1.23	1.24	0.87	0.84

Table 2: Comparison of 300 rocks behavior at Chant Sura for the explicit and the implicit schemes.

Parameter	**Explicit**		**Implicit**	
	Mean	Standard Deviation	Mean	Standard Deviation
kinetic energy (kJ)	64.60	46.50	76.48	47.79
translational velocity (m/s)	10.74	4.58	11.64	4.45
rotational velocity (rot/s)	2.71	1.10	2.98	1.03
jump height (m)	1.07	0.85	1.10	0.84

Table 3: Comparison of the computational time for the explicit and the implicit schemes (300-rock simulation).

Simulation case		**Explicit**	**Implicit**
idealized slope (ramp)		47 s	57 s
actual slope (Chant Sura)		9 s	15 s

were carried out here, setting the same initial rock orientations and time step (0.002 s) for both the explicit and the implicit schemes. The implicit scheme gives a more concentrated run-out zone for the rocks, see the first row in Fig. 4 and the distribution of rock kinetic energy looks “smoother” when compared with the explicit scheme. Most interestingly, the implicit scheme captures well the fast rotation of the flat rock during the entire trajectory while the explicit scheme cannot reproduce the rock’s stable rotation around its major principal axis. Tab. 2 lists the mean and standard deviation values for both the numerical schemes. Finally, Tab. 3 displays the computational time recorded for the 300-rock simulations under the explicit and the implicit schemes. The implicit scheme is a bit slower in comparison to the explicit scheme, which is expected as the updating of rock rotations requires more computational effort. However, the former does respect the stability properties of rotating 3D objects, which is a key improvement for RAMMS::ROCKFALL. Future simulations will be carefully validated against the real rockfall events and experiments. It is anticipated that for extremely long rolling phases of platy rocks the differences between the explicit and the implicit schemes could be even larger.

Conclusions

In this paper an extended intermediate axis theorem has been proven using Lyapunov functions. Using the same Lyapunov functions, we have given a rigorous proof that the implicit scheme presented in [5] respects the extended intermediate axis theorem. The computational cost per time-step is larger for the implicit scheme than the explicit scheme, as Newton iterations are needed to solve the implicit equations. However, numerical simulations show that the implicit scheme is far more accurate as it respects both the energy conservation and the invariance of the spin. The implicit scheme therefore allows to take larger time-steps without excessive error, making it a suitable scheme for 3D rockfall simulation.
Numerical simulations with RAMMS::ROCKFALL using the newly developed implicit scheme show that for the downward motion of a platy rock on an actual slope the rotation around the major principal axis is stable, even in the presence of intermediate collisions and contact phases with the slope. This is in correspondence with data from field experiments.

Acknowledgement

The authors are indepted to Marc Christen and Andrin Caviezel of the WSL Institute for Snow and Avalanche Research SLF for support with the RAMMS::ROCKFALL simulations and visualization.

References

[1] CAVIEZEL, A., DEMMEL, S., RINGENBACH, A., BÜHLER, Y., LU, G., CHRISTEN, M., DINNEEN, C., EBERHARD, L., VON RICKENBACH, D., AND BARTELT, P. Reconstruction of four-dimensional rockfall trajectories using remote sensing and rock-based accelerometers and gyroscopes. *Earth Surface Dynamics 7*, 1 (2019), 199–210.

[2] CHRISTEN, M., BÜHLER, Y.AND BARTELT, P., LEINE, R., GLOVER, J., SCHWEIZER, A., GRAF, C., MCARDELL, B., GERBER, W., DEUBELBEISS, Y., FEISTL, T., AND VOLKWEIN, A. Integral hazard management using a unified software environment: numerical simulation tool "RAMMS" for gravitational natural hazards. In *Proceedings 12th Congress INTERPRAEVENT* (2012), G. Koboltschnig, J. Hübl, and J. Braun, Eds., vol. 1, pp. 77–86.

[3] LEINE, R. I., SCHWEIZER, A., CHRISTEN, M., GLOVER, J., BARTELT, P., AND GERBER, W. *Multibody System Dynamics 32* (2014), 241–271.

[4] LU, G., CAVIEZEL, A., CHRISTEN, M., DEMMEL, S., RINGENBACH, A., BÜHLER, Y., DINNEEN, C., GERBER, W., AND BARTELT, P. Modelling rockfall impact with scarring in compactable soils. *Landslides* (2019), 2353–2367.

[5] SCHWEIZER, A. *Ein nichtglattes mechanisches Modell für Steinschlag*. PhD thesis, ETH Zurich, 2015.

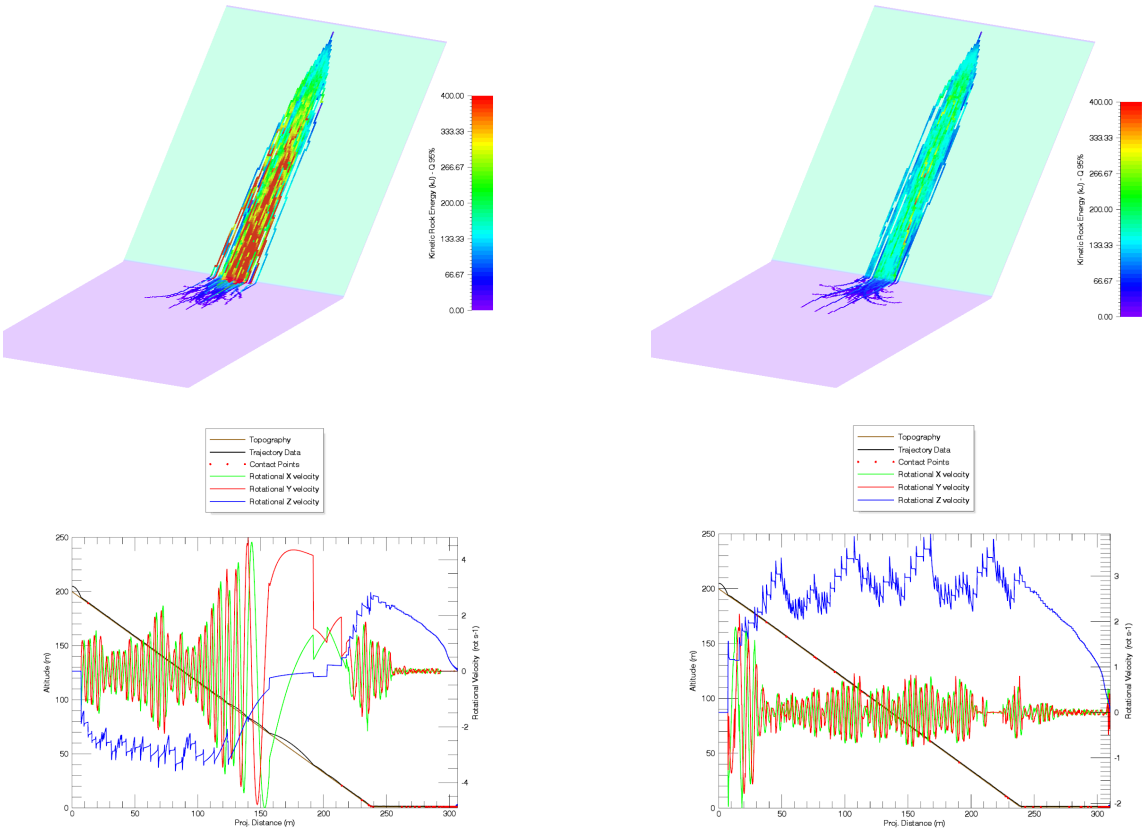

Figure 3: Disk-shaped rock rolling down an idealized inclined slope: left the explicit scheme, right the implicit scheme.

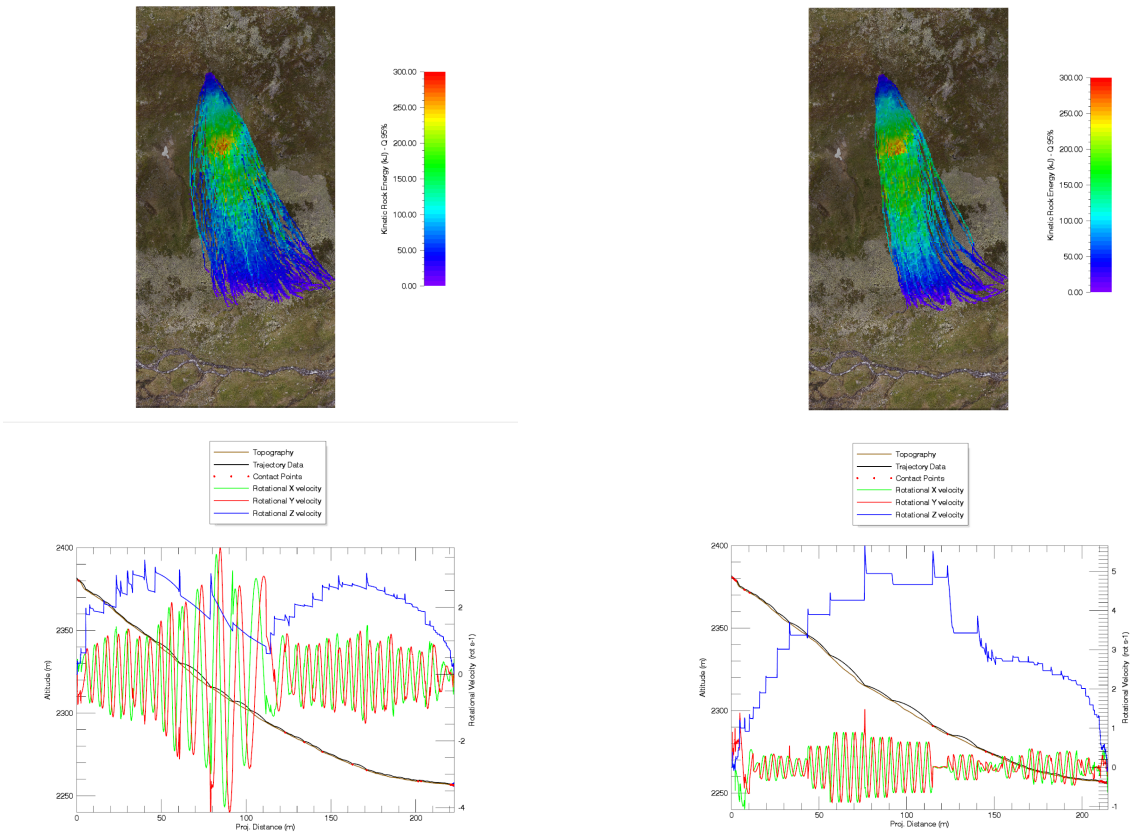

Figure 4: EOTA-shaped rock rolling down an actual slope at Chant Sura (Davos, Switzerland): left the explicit scheme, right the implicit scheme